Tight-binding electron–phonon coupling and band renormalization in graphene*

Zhang De-Sheng(张德生)[a)b)†], Kang Guang-Zhen(康广震)[b)], and Li Jun(李 俊)[a)b)]

[a)] National Laboratory of Solid State Microstructures, Nanjing University, Nanjing 210093, China
[b)] Department of Physics, Nanjing University, Nanjing 210093, China

(Received 2 July 2014; revised manuscript received 29 August 2014; published online 14 November 2014)

The kink structure in the quasiparticle spectrum of electrons in graphene observed at 200 meV below the Fermi level by angle-resolved photoemission spectroscopy (ARPES) was claimed to be caused by a tight-binding electron–phonon (e–ph) coupling in the previous theoretical studies. However, we numerically find that the e–ph coupling effect in this approach is too weak to account for the ARPES data. The former agreement between this approach and the ARPES data is due to an enlargement of the coupling constant by almost four times.

Keywords: graphene, electron–phonon interaction, kink, effective mass-renormalization parameter

PACS: 73.22.Pr, 71.10.–w, 71.18.+y, 71.38.–k **DOI:** 10.1088/1674-1056/24/1/017301

1. Introduction

The first realization of graphene[1] has inspired tremendous interest in physics both experimentally and theoretically. Graphene consists of a monolayer of carbon atoms in a honeycomb lattice which comprises two interpenetrating triangular sublattices. The band structure of graphene was first written down by Wallace.[2] A charge carrier in graphene is described by Weyl's equation in the vicinity of the Dirac point, and possesses a simple linear energy spectrum.[3] This peculiar band structure has been confirmed by angle-resolved photoemission spectroscopy (ARPES) measurements.[4] In the ARPES measurements, a kink was observed at about 200 meV below the Fermi level.[4–7] In order to explain this feature, many theories have been proposed.[8–12]

A continuum model suitable for the description of a phonon in graphene was developed,[13] upon which the coupling between electron and optical phonon was studied.[14,15] A theory for the analytical calculation of the effect of the electron–phonon (e–ph) coupling on the electronic properties of graphene was developed by Tse and Das Sarma.[10] However, the kink structure they presented was not consistent with that in the ARPES study.[4,5] Kang *et al.* revisited the approach and gave results that were more consistent with the ARPES experimental data and first-principle calculations.[12] Note that a dimensionless phonon-mediated e–e coupling constant $g_{ee}^2 = 0.02$ [10] was adopted in both calculations, the value of which was relevant to the strength of the kink structure. However, according to the definition of g_{ee}^2 in Ref. [10], the g_{ee}^2 calculated is four times smaller than 0.02. This renders the above agreement uncertain.

In this paper, we investigate the e–ph coupling in graphene due to the lattice vibration modulation of the nearest hopping energy in the tight-binding model. From the tight-banding model in second-quantized form, we formulate the e–ph coupling, from which the electron self-energy of graphene is obtained. A similar approach was adopted to calculate the conductivity of graphene[16,17] and the transport of an electron in bilayer graphene[18] taking into account the effect of the e–ph coupling. Besides, we adopt the full energy dispersion of free graphene instead of the linear energy spectrum, which is valid only in the vicinity of the Dirac point and usually used in the previous theoretical calculations. We numerically calculate the electron self-energy and the effect of the e–ph coupling to the spectral function of a quasiparticle in electron-doped graphene. We also calculate the effective mass-renormalization parameter λ_{ph}^{eff}. All our results are compared with the results of Kang *et al.* based on the Tse and Das Sarma model with $g_{ee}^2 = 0.02$,[12] and the distinction is significant. Furthermore, we also revisit Tse and Das Sarma's model by setting $g_{ee}^2 = 0.01$ for comparison.

2. Electron–phonon coupling due to the nearest hopping energy

The tight-binding model considering only the nearest neighbor hopping reads[3]

$$H = -\sum_{i,\delta} t(\boldsymbol{a}_i^\dagger \boldsymbol{b}_{i+\delta} + \boldsymbol{b}_{i+\delta}^\dagger \boldsymbol{a}_i), \tag{1}$$

where $\boldsymbol{i}$ runs over sites in sublattice A, $\boldsymbol{\delta}$ is the nearest-neighbor vector, and t is the nearest hopping energy. Since

*Project supported by the National Natural Science Foundation of China (Grant Nos. 10574063, 11275097, 10935001, 11274166, and 11075075), the National Basic Research Program of China (Grant No. 2012CB921504), and the Research Fund for the Doctoral Program of Higher Education, China (Grant No. 2012009111002).

†Corresponding author. E-mail: zhangdesheng99@gmail.com

© 2015 Chinese Physical Society and IOP Publishing Ltd

the lattice vibration changes the distance between the nearest neighbor carbon atoms, t is modulated as[14]

$$-t = -t_0 + \left(-\frac{\partial t_0}{\partial a_c}\right)\frac{1}{a_c}\boldsymbol{\delta}\cdot[\boldsymbol{u}_B(\boldsymbol{i}+\boldsymbol{\delta}) - \boldsymbol{u}_A(\boldsymbol{i})], \quad (2)$$

where $\boldsymbol{u}_A(\boldsymbol{i})$ and $\boldsymbol{u}_B(\boldsymbol{i}+\boldsymbol{\delta})$ are the lattice displacements at sublattices A and B, respectively, and $t_0 = 3.03$ eV[15] and $a_c = 1.42$ Å[3] are the nearest hopping energy and the equilibrium bond length between adjacent carbon atoms in free graphene without lattice vibration, respectively.

Only considering the long wavelength optical phonon, we have[14]

$$\boldsymbol{u}_B(\boldsymbol{r}+\boldsymbol{\delta}) - \boldsymbol{u}_A(\boldsymbol{r}) \approx \sqrt{2}\boldsymbol{u}(\boldsymbol{r}), \quad (3)$$

where $\boldsymbol{u}(\boldsymbol{r})$ is the relative displacement corresponding to the optical phonon. We shall focus on the coupling between electron and longitudinal phonon in graphene. For the long wavelength optical phonon,[15]

$$\boldsymbol{u}(\boldsymbol{r}) = \sqrt{\frac{\hbar}{2NM_c\omega_0}}\sum_{\boldsymbol{q}}(A_{\boldsymbol{q}} + A^{\dagger}_{-\boldsymbol{q}})\boldsymbol{e}(\boldsymbol{q})e^{i\boldsymbol{q}\cdot\boldsymbol{r}}, \quad (4)$$

where N is the number of unit cells, $\hbar\omega_0 = 196$ meV is the optical phonon frequency at the Γ point of graphene, $M_c = 1.993\times10^{-23}$ g is the mass of a carbon atom, and $A_{\boldsymbol{q}}$ and $A^{\dagger}_{-\boldsymbol{q}}$ are the destruction and the creation operators of a phonon, respectively. For the longitudinal phonon,

$$\boldsymbol{e}(\boldsymbol{q}) = i(q_x, q_y)/q. \quad (5)$$

Substituting Eqs. (2)–(4) into Eq. (1) and using the Fourier transform

$$\boldsymbol{a}_{\boldsymbol{i}} = \frac{1}{\sqrt{N}}\sum_{\boldsymbol{k}} a_{\boldsymbol{k}}e^{i\boldsymbol{k}\cdot\boldsymbol{i}}, \quad b_{\boldsymbol{i}+\boldsymbol{\delta}} = \frac{1}{\sqrt{N}}\sum_{\boldsymbol{k}} b_{\boldsymbol{k}}e^{i\boldsymbol{k}\cdot(\boldsymbol{i}+\boldsymbol{\delta})}, \quad (6)$$

we can obtain

$$H = H_0 + H_1. \quad (7)$$

The first term is the tight-binding model Hamiltonian for free graphene without lattice vibration

$$H_0 = \sum_{\boldsymbol{k}}\psi^{\dagger}_{\boldsymbol{k}}\begin{pmatrix}0 & \gamma_{\boldsymbol{k}}\\ \gamma^*_{\boldsymbol{k}} & 0\end{pmatrix}\psi_{\boldsymbol{k}}, \quad (8)$$

where

$$\gamma_{\boldsymbol{k}} = -t_0\sum_{\boldsymbol{\delta}}e^{i\boldsymbol{k}\cdot\boldsymbol{\delta}}, \quad (9)$$

and $\psi_{\boldsymbol{k}} = [a_{\boldsymbol{k}}\ b_{\boldsymbol{k}}]^T$ is a two-component operator.

The second term represents the e–ph coupling

$$H_1 = \frac{g_{ep}}{\sqrt{N}}\sum_{\boldsymbol{k},\boldsymbol{q}}\psi^{\dagger}_{\boldsymbol{k}}\boldsymbol{M}(\boldsymbol{k},\boldsymbol{q})\psi_{\boldsymbol{k}-\boldsymbol{q}}(A_{\boldsymbol{q}} + A^{\dagger}_{-\boldsymbol{q}}), \quad (10)$$

where $\boldsymbol{M}(\boldsymbol{k},\boldsymbol{q})$ is the coupling matrix between electron and phonon

$$\boldsymbol{M}(\boldsymbol{k},\boldsymbol{q}) = \frac{1}{a_c}\sum_{\delta}\begin{pmatrix}0 & (\boldsymbol{\delta}\cdot\boldsymbol{e}(\boldsymbol{q}))e^{i(\boldsymbol{k}-\boldsymbol{q})\cdot\boldsymbol{\delta}}\\ (\boldsymbol{\delta}\cdot\boldsymbol{e}(\boldsymbol{q}))e^{-i\boldsymbol{k}\cdot\boldsymbol{\delta}} & 0\end{pmatrix}, \quad (11)$$

and

$$g_{ep} = \frac{\beta t_0}{a_c}\sqrt{\frac{\hbar}{M_c\omega_0}} \quad (12)$$

gives the magnitude of the e–ph coupling, with $\beta = -d\ln t_0/d\ln a_c \sim 2$.[15]

Diagonalizing H_0 and considering the chemical potential, we can obtain the full energy dispersion of free graphene

$$\xi_{\lambda}(\boldsymbol{k}) = \lambda|\gamma_{\boldsymbol{k}}| - \mu, \quad (13)$$

where $\lambda = +1$ and -1 correspond to the conduction and the valance bands, respectively, and μ is the chemical potential.

Note that we adopt the full energy dispersion expressed in Eq. (13) rather than the linear dispersion, which is valid in the vicinity of the Dirac point and usually used in the previous theoretical calculations,[10,12] so our current model is working in a different basis representation. Both coupling matrix and coupling constant have different meanings from those in Ref. [10]. In fact, $g^2_{ep} = 0.033\,\text{eV}^2$ in our current model.

Using Green's function theory, we obtain the expression for the electron self-energy due to the e–ph coupling in the diagonal basis

$$\begin{aligned}\Sigma_{\pm}(\boldsymbol{k}, i\omega_n) = -\frac{g^2_{ep}}{2\beta_T}\frac{1}{N}\sum_{\boldsymbol{q},i\omega_m}\sum_{\lambda}\mathcal{G}^{(0)}_{\lambda}(\boldsymbol{k}-\boldsymbol{q}, i\omega_n - i\omega_m)\\ \times\mathcal{D}^{(0)}(i\omega_m)[(|M_{12}(\boldsymbol{k},\boldsymbol{q})|^2 + |M_{21}(\boldsymbol{k},\boldsymbol{q})|^2)/2\\ \pm\lambda\,\text{Re}(M_{12}(\boldsymbol{k},\boldsymbol{q})^* M_{21}(\boldsymbol{k},\boldsymbol{q})e^{i(\theta_{\boldsymbol{k}}+\theta_{\boldsymbol{k}-\boldsymbol{q}})})], \quad (14)\end{aligned}$$

where $\mathcal{G}^{(0)}_{\lambda}(\boldsymbol{k}, i\omega_n) = 1/[i\omega_n - \xi_{\lambda}(\boldsymbol{k})]$ is the electron Green's function of free graphene in the diagonal basis, $\mathcal{D}^{(0)}(i\omega_m) = 2\hbar\omega_0/[(i\omega_m)^2 - (\hbar\omega_0)^2]$ is the free phonon Green's function, and $e^{i\theta_{\boldsymbol{k}}} = \gamma_{\boldsymbol{k}}/|\gamma_{\boldsymbol{k}}|$. Because we now work with a complex nonlinear energy dispersion, we are not able to obtain an analytical expression of the self-energy through integrating over $\boldsymbol{q}$. The self-energy can only be calculated numerically.

A similar approach to formulate the self-energy due to the e–ph coupling in graphene was employed in the previous works,[16,17] however, some technical differences need to be mentioned here. Firstly, in those previous works, the free electron Green's function in the expression of the self-energy is corresponding to the operator $\psi_{\boldsymbol{k}}$, and is not identified with $\mathcal{G}^{(0)}_{\lambda}(\boldsymbol{k}, i\omega_n)$ in Eq. (14). Secondly, the integral over momentum $\boldsymbol{q}$ is performed by adopting the linear energy dispersion and introducing a cut-off energy.

3. Results and discussion

In Tse and Das Sarma's approach, the e–ph coupling constant is[10]

$$g = -\frac{\beta\hbar v_{\rm F}}{a_{\rm c}^2}\sqrt{\frac{\hbar}{2NM_{\rm c}\omega_0}}, \tag{15}$$

where $v_{\rm F} = 3a_{\rm c}t_0/(2\hbar)$ is the Fermi velocity of the Dirac fermion.[3] They defined the dimensionless coupling constant[10]

$$g_{\rm ee}^2 \equiv \frac{g^2\mathcal{A}}{\hbar^2 v_{\rm F}^2}, \tag{16}$$

where $\mathcal{A}$ is the area of the graphene sample. Accordingly, we find $g_{\rm ee}^2 = 0.0046$. Thus, the value of $g_{\rm ee}^2$ fixed by the atomic parameters in graphene is four times smaller than 0.02, which was adopted by Tse and Das Sarma as well as Kang *et al.*[10,12]

In Fig. 1, we present the real and the imaginary parts of the electron self-energy at doping $n = 1.0\times10^{13}$ cm^{-2}. The black solid line is the result numerically calculated from Eq. (14), and the blue dashed line is that of Tse and Das Sarma's model with $g_{\rm ee}^2 = 0.02$.[12] The difference between the two results is remarkable. The mutation of the real part and the jump of the imaginary part of the self-energy at $-\omega_0$ obtained in our current model are much weaker than those in Tse and Das Sarma's model.[10,12] The self-energy in our results is smaller. We also calculate the self-energies at doping levels $n = 4.5\times10^{13}$ cm^{-2} and 12.0×10^{13} cm^{-2}, and find that this difference becomes larger with increasing doping. The real and the imaginary parts of the self-energy control the energy renormalization and the broadening of the spectral of quasiparticles. So the energy spectrum renormalization due to the e–ph coupling in our current model will be much weaker.

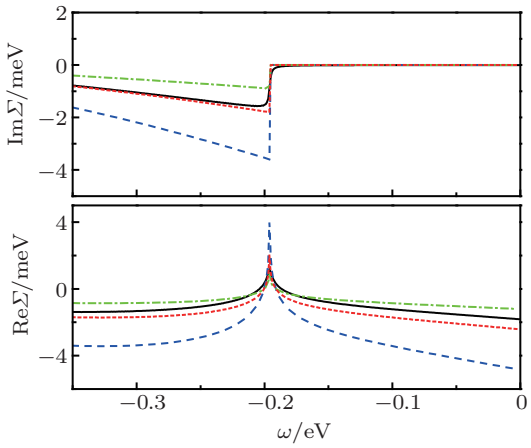


Fig. 1. (color online) Real and imaginary parts of the self-energy of graphene with electron-phonon coupling at $\boldsymbol{k} = \boldsymbol{k}_{\rm F}$. The doping is $n = 1.0\times10^{13}$ cm^{-2}. The solid (black) curve is the results of our current model. The dashed (blue), the short-dashed (red), and the dot-dashed (green) curves are the results of Tse and Das Sarma's model with $g_{\rm ee}^2 = 0.02$, 0.01, and 0.005, respectively.

Such a big difference is unacceptable, because the origin of the e–ph coupling we considered and the atomic parameters we used are exactly the same as those of Tse and Das Sarma. As we mentioned above, the value of $g_{\rm ee}^2 = 0.02$ in Tse and Das Sarma's approach is overstated. For comparison, we calculate the electron self-energy using Tse and Das Sarma's model with $g_{\rm ee}^2 = 0.005$ and 0.01 respectively. In Fig. 1, the green dot-dashed curve is for $g_{\rm ee}^2 = 0.005$ and the red short-dashed curve is for $g_{\rm ee}^2 = 0.01$. The results from Tse and Das Sarma's model with $g_{\rm ee}^2 = 0.005$ become too small to be consistent with our model. It is interesting that the result with $g_{\rm ee}^2 = 0.01$ is very close to that of our current model. The similarity between the results of our current model and those of Tse and Das Sarma's model with $g_{\rm ee}^2 = 0.01$ is confirmed further at doping levels $n = 4.5\times10^{13}$ cm^{-2} and 12.0×10^{13} cm^{-2}. This implies that the appropriate value of $g_{\rm ee}^2$ in Tse and Das Sarma's model should be about 0.01.

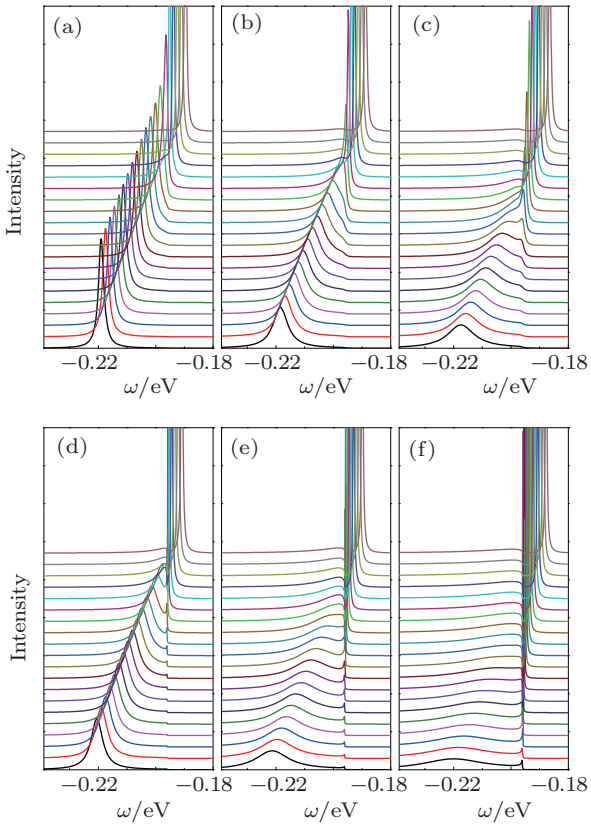


Fig. 2. (color online) EDCs in a narrow $\boldsymbol{k}$ range near the kink structure at doping levels (a), (d) 1.0×10^{13} cm^{-2}; (b), (e) 4.5×10^{13} cm^{-2}; and (c), (f) 12.0×10^{13} cm^{-2}. Panels (a)–(c) are results of our current model, while panels (d)–(f) are those of Tse and Das Sarma's model with $g_{\rm ee}^2 = 0.02$.

The spectral function is a central quantity in a many-body system, which is expressed in terms of the self-energy as

$$A_\lambda(\boldsymbol{k},\omega) = -\frac{1}{\pi}{\rm Im}\frac{1}{\omega - \xi_\lambda(\boldsymbol{k}) - \Sigma_\lambda(\boldsymbol{k},\omega)}. \tag{17}$$

The energy distribution curve (EDC), a plot of $A(\boldsymbol{k},\omega)$ versus ω for a fixed value of $\boldsymbol{k}$, reveals the energy renormalization of the quasiparticle.

In Fig. 2, a set of EDCs in a narrow $\boldsymbol{k}$ range around the kink structure at different doping levels $n = 1.0 \times 10^{13}$ cm^{-2}, 4.5×10^{13} cm^{-2}, and 12.0×10^{13} cm^{-2} is shown. From bottom to top in every group of EDCs, $\boldsymbol{k}$ is approaching Fermi momentum $\boldsymbol{k}_{\rm F}$. Figures 2(a)–2(c) are the results of our current calculations. At doping $n = 1.0 \times 10^{13}$ cm^{-2}, all the EDCs almost exhibit single-particle peaks with fine Lorentzian forms as expected for a free Landau fermion. The kink structure is hardly noticeable. With increasing doping, a double-peak structure appears in the EDCs, and the second peak emerges at about $-\omega_0$. From bottom to top, the first peak is moving toward $\omega = -\omega_0$ and becomes lower and broader, while the second peak pinning at $-\omega_0$ becomes more important and finally dominates in the EDC. The evolution of the weakening of the first peak and the enhancing of the second peak results in the kink structure. The description in terms of quasiparticle is not reliable in the range of the kink structure. The distance between the two peaks describes the range of the kink. The larger the doping level, the larger the range of the kink structure. We also show the results obtained by Kang *et al.* from Tse and Das Sarma's model with $g_{\rm ee}^2 = 0.02$ [12] in Fig. 2 for comparison. The kink structure is obviously sharper and larger than that obtained in our current model. The kink is already noticeable at small doping $n = 1.0 \times 10^{13}\,{\rm cm}^{-2}$. This large magnitude of the kink is relevant to the large $g_{\rm ee}^2$. We believe that the kink structure will become much smaller and approach the feature of our current model if $g_{\rm ee}^2 = 0.01$.

In Fig. 3, the momentum distribution curves (MDCs) for given energies -214 meV, -206 meV, -186 meV, and -174 meV are presented. The MDCs can be described by a single Lorentzian peak. The peak is very sharp between the kink and the Fermi level because the imaginary part of the self-energy is almost zero in this energy range. The MDCs width increase significantly below the kink due to the sudden increase of the imaginary part of the self-energy.[19] The peak becomes broader with increasing electron doping. This means that the renormalization is stronger for a larger doping level.

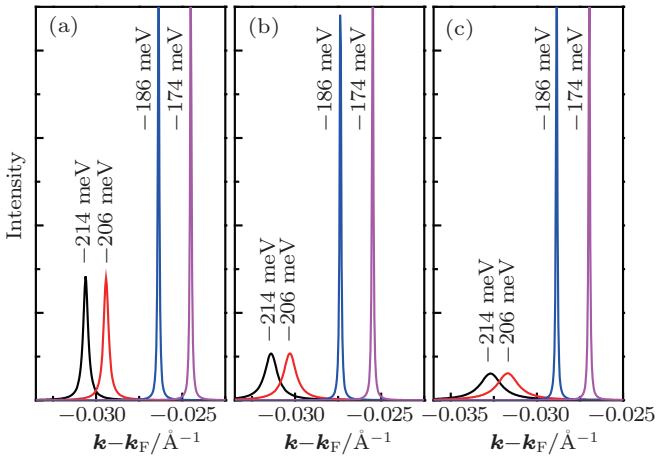


Fig. 3. (color online) MDCs for given energies at doping levels (a) 1.0×10^{13} cm^{-2}, (b) 4.5×10^{13} cm^{-2}, and (c) 12.0×10^{13} cm^{-2}.

In Fig. 4(a), we plot the magnitude of the spectral function of graphene calculated from Eq. (17) at three doping levels $n = 1.0 \times 10^{13}$ cm^{-2}, 4.5×10^{13} cm^{-2}, and 12.0×10^{13} cm^{-2}. We also give the renormalized dispersion of the quasiparticle by connecting the maximum peak positions of the EDCs. At doping $n = 1.0 \times 10^{13}$ cm^{-2}, the renormalized dispersion almost coincides with that of bare graphene, and the kink structure is hardly recognized. At larger doping 4.5×10^{13} cm^{-2} or 12.0×10^{13} cm^{-2}, a kink structure appears in the vicinity of $-\omega_0$, and the renormalized dispersion deviates from the bare unrenormalized dispersion.

Compared with Tse and Das Sarma's results, the shape of the kink obtained in Kang's work is qualitatively similar to those in Refs. [20] and [21]. In Fig. 4(b), we present the corresponding results that Kang *et al.* calculated from Tse and Das Sarma's model with $g_{\rm ee}^2 = 0.02$.[12] The distinction between the top and bottom panels in Fig. 2 is clearly revealed in Fig. 4. It is obvious that the shapes of the kink structure calculated from the two models are similar. However, the sharpness and the range of the kink in our current results are much smaller. The kink range is about 10 meV and 15 meV at the doping levels of 4.5×10^{13} cm^{-2} and 12.0×10^{13} cm^{-2}, respectively, which are smaller than 25 meV and 45 meV in Ref. [12]. Out of the range of the kink, the deviation of the renormalized spectrum from the bare spectrum in our current model is also much smaller. These disagreements are owing to the overstated value of $g_{\rm ee}^2$. So we revisit Tse and Das Sarma's model by setting $g_{\rm ee}^2 = 0.01$, and present the results in Fig. 5. Comparing with Fig. 4(a), We find that all the features of the results are now very consistent with those of our current model. These suggest that the e–ph coupling due to the nearest hopping energy is not strong enough to explain the kink structure observed in experiments.[4–6]

In Fig. 6, the effective mass-renormalization parameters near the Fermi level $\lambda_{\rm eff}^{\rm ph} = v/v^*(\boldsymbol{k}_{\rm F}) - 1$ at three doping levels $n = 1.0 \times 10^{13}$ cm^{-2}, 4.5×10^{13} cm^{-2}, and 12.0×10^{13} cm^{-2} are presented. The renormalized Fermi velocity $v^*(\boldsymbol{k}_{\rm F})$ is obtained by linear fitting the maximum peak positions of the EDCs of several momenta near $\boldsymbol{k}_{\rm F}$. The reduction of the Fermi velocity is about 1–2% within doping range $n = 1.0 \times 10^{13}$–12.0×10^{13} cm^{-2}, which is significantly smaller than the 2–5% that Kang *et al.* obtained from Tse and Das Sarma's model with $g_{\rm ee}^2 = 0.02$.[12] However, the latter is again close to the former by setting $g_{\rm ee}^2 = 0.01$, as shown in Fig. 6. This value is much smaller than those obtained in experiments and first-principle calculations.[4,5,9] Note that the results for Tse and Das Sarma's model with $g_{\rm ee}^2 = 0.02$ in Fig. 6 are corresponding to Kang's calculations,[12] which are already smaller than Tse and Das Sarma's results.[10] Taking into account the contribution of the electron–electron Coulomb interaction $\lambda_{\rm eff}^{\rm c}$ in Refs. [22]–[24], we obtain $\lambda_{\rm eff} = \lambda_{\rm eff}^{\rm ph} + \lambda_{\rm eff}^{\rm c}$. Therefore, we conclude that the mass-renormalization parameter $\lambda_{\rm eff}$ is in the order of 7–9% within the range of doping $n = 1.0 \times 10^{13}$–12.0×10^{13} cm^{-2}.

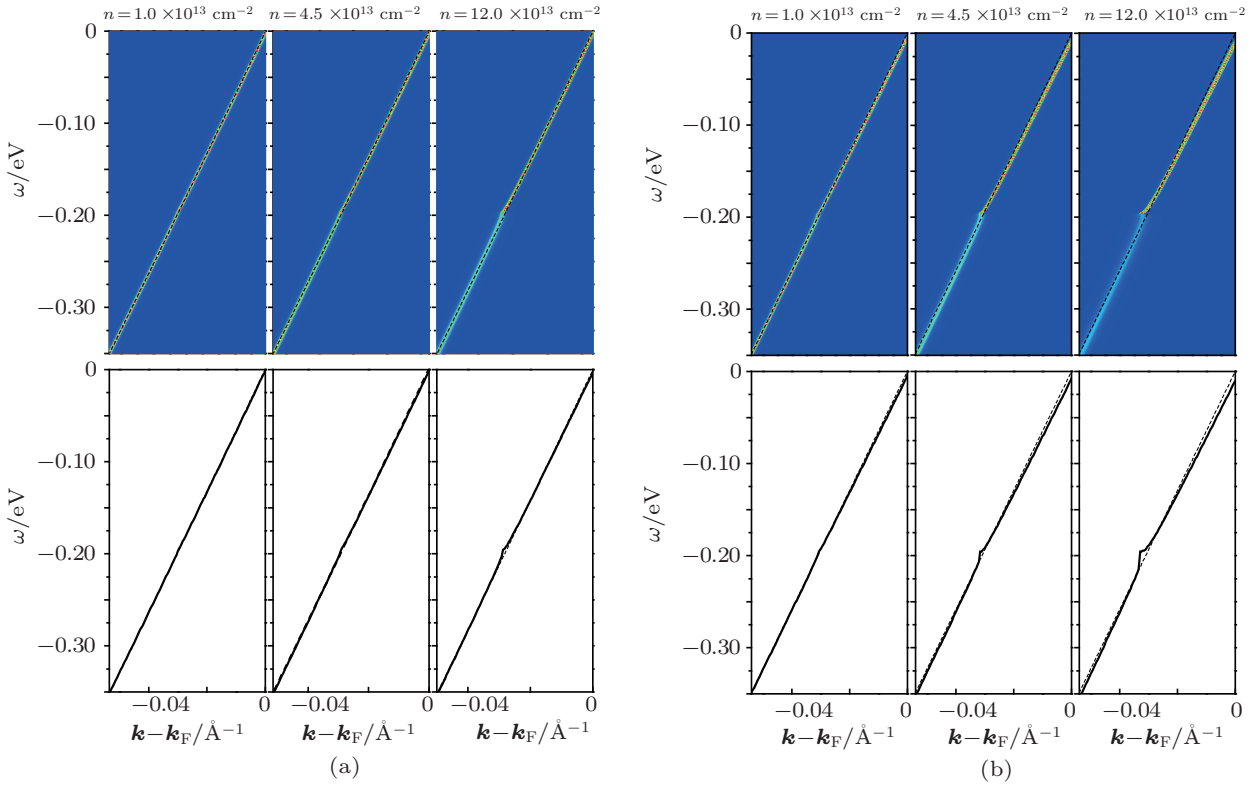


Fig. 4. (color online) The magnitude of the spectral function $A(\boldsymbol{k},\omega)$ (top panel) and the renormalized quasiparticle dispersion plotted by connecting the maximum peak positions of the EDCs (bottom panel). The dashed lines show the dispersion of free graphene. (a) The results obtained from our current model. Momentum $\boldsymbol{k}$ is along the K–Γ direction. (b) The results obtained by Kang *et al.* from Tse and Das Sarma's model with $g_{\rm ee}^2 = 0.02$.

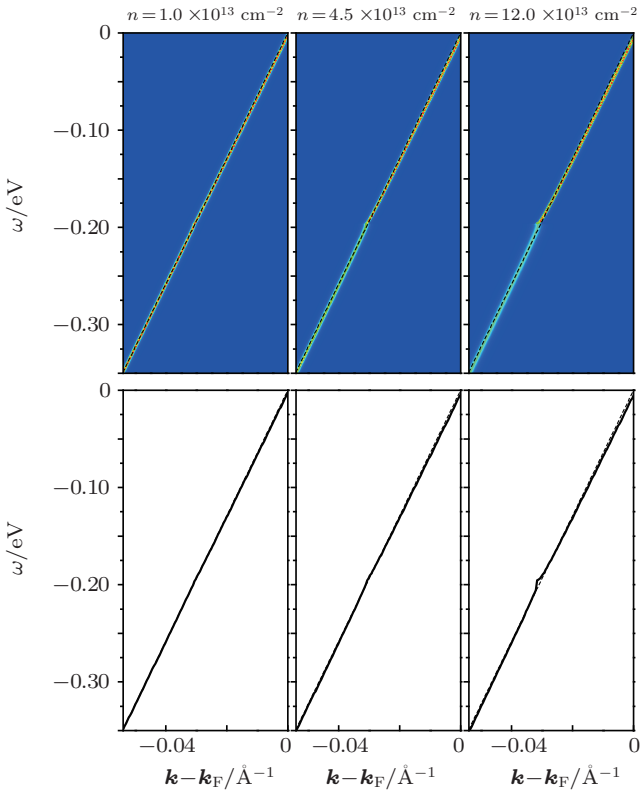


Fig. 5. (color online) The renormalized conduction-band energy spectrum calculated from Tse and Da Sarma's model with $g_{\rm ee}^2 = 0.01$. The dashed lines show the dispersion of free graphene. The top panel shows the magnitude of the spectral function $A(\boldsymbol{k},\omega)$, and the bottom panel shows the renormalized quasiparticle dispersion plotted by connecting the maximum peak positions of the EDCs.

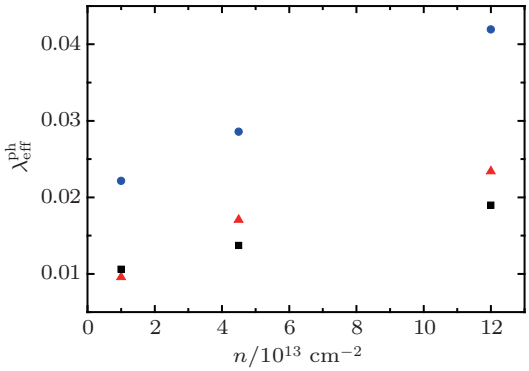


Fig. 6. (color online) The effective mass-renormalization parameter $\lambda_{\rm eff}^{\rm ph} = v/v^*(\boldsymbol{k}_{\rm F}) - 1$ at three different doping levels 1.0×10^{13} cm^{-2}, 4.5×10^{13} cm^{-2}, and 12.0×10^{13} cm^{-2}. The black square is for our current model. The blue dot and the red triangle are for Tse and Das Sarma's model with $g_{\rm ee}^2 = 0.02$ and 0.01, respectively.

4. Summary and conclusion

To summarize, we investigate the e–ph coupling due to the lattice vibration modulation of the nearest hopping energy in the tight-binding model for the kinetic energy of electrons in graphene. We numerically calculate the electron self-energy and the effect of the e–ph coupling on the spectral function of quasiparticle in electron-doped graphene. The effect of the e–ph coupling on the band structure renormalization is very slight at the low doping level $n = 1.0\times10^{13}$ cm^{-2}, and the kink is hardly recognizable. At doping levels $n = 4.5\times10^{13}$ cm^{-2} and 12.0×10^{13} cm^{-2}, a kink structure emerges

at phonon energy $\hbar\omega_0 = 196$ meV below the Fermi level. However, the sharpness and the strength of the kink are much smaller than those in the previous calculations.[10,12] Far away from the kink, the quasiparticle description is still valid, while the renormalized dispersion deviates from the bare dispersion. The mass-renormalization parameter $\lambda_{\rm eff}$ near the Fermi level is about 7–9% within the doping range $n = 1.0 \times 10^{13}$–12.0×10^{13} cm^{-2}. This value is smaller than that obtained in experiments[4,5] and theoretical calculations.[9,10,12] Comparing our results with those that Kang *et al.* obtained from Tse and Das Sarma's approach,[12] a significant difference is presented. The effect of the e–ph coupling we obtained is much weaker. This disagreement is due to the enlargement of $g_{\rm ee}^2$ in Ref. [10]. It is plausible that $g_{\rm ee}^2 = 0.01$.

In conclusion, our numerical analysis shows that the electron–phonon coupling due to the lattice vibration modulation of the nearest hopping energy as first used by Tse and Das Sarma[10] is too weak to explain the kink structure of the quasiparticle band in graphene as observed in ARPES[4–6] and first-principle calculations.[20] This result is in agreement with another theoretical work,[9] where the electron–phonon coupling matrix elements (with the electron–phonon coupling strength being fixed by *ab initio* calculations[25]) are different from those adopted in the present paper. However, there is also another kind of theoretical work[8] that claimed an agreement with the experimental data. Thus, the electron–phonon coupling scenario for the kink structure of the quasiparticle band as found in ARPES experiments needs to be studied further.

References

[1] Novoselov K S, Geim A K, Morozov S V, Jiang D, Zhang Y, Dubonos S V, Grigorieva I V and Firsov A A 2004 *Science* **306** 666
[2] Wallace P R 1947 *Phys. Rev.* **71** 622
[3] Castro Neto A H, Guniea F, Peres N M R, Novoselov K S and Geim A K 2009 *Rev. Mod. Phys.* **81** 109
[4] Bostwick A, Ohta T, Seyller T, Horn K and Rotenberg E 2007 *Nat. Phys.* **3** 36
[5] Bianchi M, Rienks E D L, Lizzit S, Baraldi A, Balog R, Hornekær L and Hofmann Ph 2010 *Phys. Rev. B* **81** 041403(R)
[6] Park C H, Giustino F, Spataru C D, Cohen M L and Louie S G 2009 *Nano. Lett.* **9** 4234
[7] Haberer D, Petaccia L, Fedorov A V, Praveen C S, Fabris S, Piccinin S, Vilkov O, Vyalikh D V, Preobrajenski A, Verbitskiy N I, Shiozawa H, Fink J, Knupfer M, Büchner B and Grüneis A 2013 *Phys. Rev. B* **88** 081401(R)
[8] Carbotte J P, Nicol E J and Sharapov S G 2010 *Phys. Rev. B* **81** 045419
[9] Calandra M and Mauri F 2007 *Phys. Rev. B* **76** 205411
[10] Tse W K and Das Sarma S 2007 *Phys. Rev. Lett.* **99** 236802
[11] Hwang E H and Das Sarma S 2008 *Phys. Rev. B* **77** 081412(R)
[12] Kang G Z, Zhang D S and Li J 2013 *Phys. Rev. B* **88** 045113
[13] Suzuura H and Ando T 2002 *Phys. Rev. B* **65** 235412
[14] Ishikawa K and Ando T 2006 *J. Phys. Soc. Jpn.* **75** 084713
[15] Ando T 2006 *J. Phys. Soc. Jpn.* **75** 124701
[16] Stauber T and Peres N M R 2008 *J. Phys: Condens. Matter* **20** 055002
[17] Stauber T, Peres N M R and Castro Neto A H 2008 *Phys. Rev. B* **78** 085418
[18] He L M 2013 *Chin. Phys. B* **22** 017201
[19] Pletikosić I, Kralj M, Milun M and Pervan P 2012 *Phys. Rev. B* **85** 155447
[20] Carbotte J P, LeBlanc J P F and Ashby Phillip E C 2013 *Phys. Rev. B* **87** 045405
[21] LeBlanc J P F, Carbotte J P and Nicol E J 2011 *Phys. Rev. B* **84** 165448
[22] Das Sarma S, Hwang E H and Tse W K 2007 *Phys. Rev. B* **75** 121406(R)
[23] Hwang E H, Ben Y K and Das Sarma S 2007 *Phys. Rev. B* **76** 115434
[24] Barlas Y, Pereg-Barnea T, Polini M, Asgari R and MacDonald A H 2007 *Phys. Rev. Lett.* **98** 236601
[25] Piscanec S, Lazzeri M, Mauri F, Ferrari A C and Robertson J 2004 *Phys. Rev. Lett.* **93** 185503